Quaternary Science Reviews 112 (2015) 197–206

Contents lists available at ScienceDirect

Quaternary Science Reviews

journal homepage: www.elsevier.com/locate/quascirev

Persistently strong Indonesian Throughflow during marine isotope stage 3: evidence from radiogenic isotopes

Roland Stumpf [a, b, *], Steffanie Kraft [a], Martin Frank [a], Brian Haley [a, 1], Ann Holbourn [c], Wolfgang Kuhnt [c]

[a] GEOMAR Helmholtz Centre for Ocean Research Kiel, Wischhofstraße 1-3, 24148 Kiel, Germany
[b] Department of Earth Science & Engineering, Imperial College London, SW7 2AZ London, UK
[c] Institute of Geoscience, Christian Albrechts University Kiel, 24118 Kiel, Germany

ARTICLE INFO

Article history:
Received 24 February 2014
Received in revised form
23 December 2014
Accepted 28 January 2015
Available online

Keywords:
Indonesian Throughflow
Neodymium isotopes
Lead isotopes
Strontium isotopes
Marine isotope stage 3
Ferromanganese coatings
Foraminiferal cleaning

ABSTRACT

The Indonesian Throughflow (ITF) connects the western Pacific Ocean with the eastern Indian Ocean, thus forming one of the major near surface current systems of the global thermohaline circulation. The intensity of the ITF has been found to be sensitive to changes in global ocean circulation, fluctuations in sea level, as well as to the prevailing monsoonal conditions of the Indonesian Archipelago and NW Australia. This study presents the first reconstruction of ITF dynamics combining radiogenic isotope compositions of neodymium (Nd), strontium (Sr), and lead (Pb) of the clay-size detrital fraction to investigate changes in sediment provenance, and paleo seawater Nd signatures extracted from the planktonic foraminifera and authigenic Fe–Mn oxyhydroxide coatings of the marine sediments focussing on marine isotope stage 3 (MIS3). Sediment core MD01-2378 was recovered within the framework of the International Marine Global Change Study (IMAGES) and is located in the area of the ITF outflow in the western Timor Sea (Scott Plateau, 13° 04.95′ S and 121° 47.27′ E, 1783 m water depth). In order to produce reliable seawater signatures, several extraction methods were tested against each other. The results of the study show that at this core location the extraction of surface water Nd isotope compositions from planktonic foraminifera is complicated by incomplete removal of contributions from Fe–Mn oxyhydroxides carrying ambient bottom water signatures. The bottom water Nd isotope signatures reliably obtained from the sediment coatings (average $\varepsilon Nd = -5.0$) document an essentially invariable water mass composition similar to today throughout the entire MIS3. The radiogenic Nd, Sr, and Pb isotope records of the clay-sized detrital fraction suggest that the Indonesian Archipelago rather than NW Australia was the main particle source at the location of core MD01-2378, and thus indicating a persistently strong ITF during MIS3. Furthermore, the variations of the detrital radiogenic isotopes are shown to be more sensitive to changes in circulation and document a somewhat enhanced ITF intensity during the early part of MIS3 until 47.4 ka compared with the remaining MIS3.

1. Introduction

The Indonesian Throughflow (ITF) defines the hydrographic gateway between the Pacific and Indian Oceans. Hence, it constitutes one of the key areas for present-day global ocean exchange processes (e.g., salinity, heat), as well as a sensitive location for climatic and environmental changes through time (Visser et al., 2003; Ruth et al., 2007).

The ITF current system forms a major part of the surface water pathways of the global thermohaline circulation and is characterized by low-salinity surface and intermediate waters from the western and northwestern Pacific Ocean flowing through the Indonesian Archipelago and entering the eastern Indian Ocean (Schmitz, 1995; Gordon, 2005; Xu et al., 2010). The Pacific surface and subsurface waters enter the Indonesian Archipelago south of the Philippines and pass the Celebes Sea and Makassar Strait southwards into the eastern Java Sea (Fig. 1). While a part of these

* Corresponding author. Department of Earth Science & Engineering, Imperial College London, SW7 2AZ London, UK. Tel.: +44 (0)20 759 46486.
E-mail address: r.stumpf@imperial.ac.uk (R. Stumpf).
[1] Now at: College of Earth, Ocean & Atmospheric Sciences, Oregon State University, Corvallis, OR 97331-5503, USA.

http://dx.doi.org/10.1016/j.quascirev.2015.01.029
0277-3791/

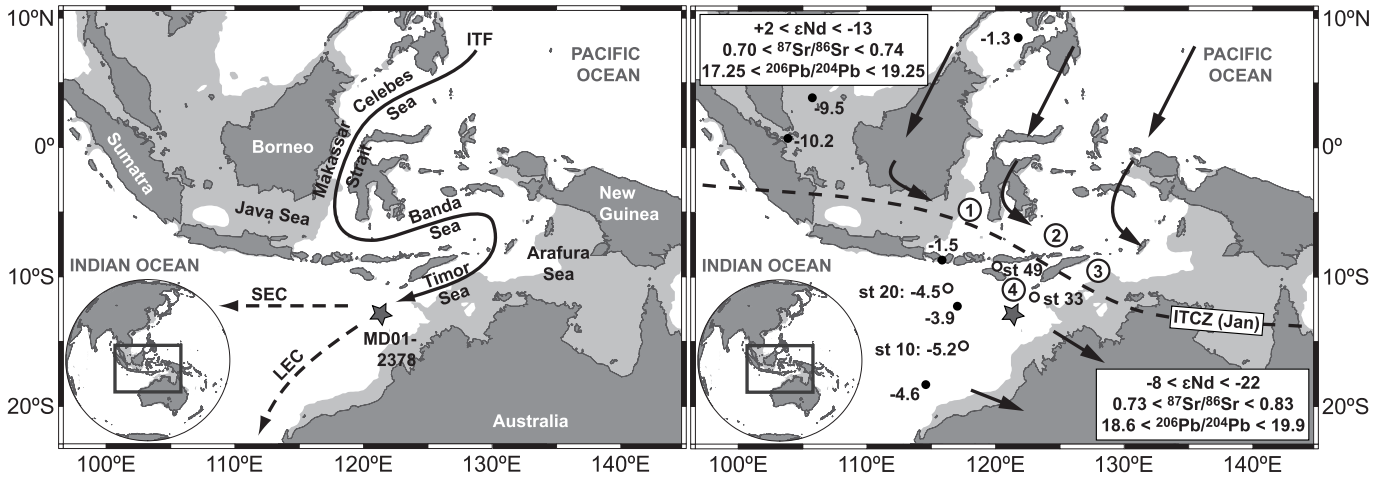

Fig. 1. (left): The Indonesian Seas with the main pathway of the Indonesian Throughflow (ITF) and proximal ocean currents, as well as the location of sediment core MD01-2378 (star symbol) in the western Timor Sea (modified from Godfrey, 1996; Spooner et al., 2005; Zuraida et al., 2009; SEC: South Equatorial Current; LEC: Leeuwin Current). The area shaded in grey denotes the coastline at a sea level 100 m lower than today corresponding to the minimum levels reached during MIS3. (right): Nd isotope compositions of surface (solid dots) and subsurface (open dots) waters (Jeandel et al., 1998; Amakawa et al., 2000), and the range of radiogenic Nd, Sr, Pb isotope compositions of Indonesian (upper left box) and NW Australian (lower right box) source rocks (Vroon et al., 1995). Numbers 1–4 refer to locations of surface sediments along the ITF pathway (Ehlert et al., 2011). Arrows indicate simplified wind trajectories during NW monsoon conditions in Austral summer, the dashed line shows the corresponding approximate position of the ITCZ in January (e.g., Gingele et al., 2002; Xu et al., 2008). Note: During Austral winter, the ITCZ is located at 10–15°N (outside the map margins) and easterly winds of the SE monsoon predominate in the Indonesian Seas.

waters exits directly southwards into the eastern Indian Ocean through the Lombok Strait, the main pathway of the ITF continues eastwards into the Banda Sea (Godfrey, 1996). In addition, there are some minor contributions of Pacific surface waters reaching the Banda Sea from the north through the Halmahera and Molucca Seas (Spooner et al., 2005). Regional excess of precipitation over evaporation, vertical mixing, as well as freshwater contributions from the South China Sea lead to a salinity decrease within the Banda Sea to levels lower than those of the Pacific source waters (Hautala et al., 1996; Tozuka et al., 2009). Finally, the modified ITF surface waters exit the Banda Sea into the eastern Indian Ocean via the Ombai and the Timor Straits of the Timor Sea.

The ITF waters branch out westwards and contribute to the South Equatorial Current (SEC), which crosses the Indian Ocean and has an impact on the strength and hydrographic properties of the Agulhas Current. A second branch of the ITF heads southwards to strengthen the Leeuwin Current flowing along the west coast of Australia (Godfrey, 1996). These large scale current systems directly respond to changes in ITF intensity, which itself is strongly influenced by the prevailing atmospheric conditions over Asia and Australia (Godfrey, 1996; Wijffels et al., 1996; Gordon, 2005; Spooner et al., 2005; Schott et al., 2009). Specifically, the intensity and volume flow of the ITF within the Indonesian Archipelago respond significantly to the regional monsoonal system. During Austral winter (May–September) when the Inter Tropical Convergence Zone (ITCZ) is located at about 10–15°N, westward blowing winds of the SE monsoon promote an intensification of the ITF accompanied by a shallowing of the surface mixed layer. In contrast, during Austral summer (November–March) the ITCZ shifts southward and eastward winds of the NW monsoon accumulate water in the Banda Sea resulting in a deepening of the thermocline, as well as in a decrease of ITF intensity (Wijffels et al., 1996; Gordon, 2005; Fig. 1).

The reconstruction of past variations in ITF intensity thus can serve to draw conclusions about regional and global oceanic and climatic conditions. Previous reconstructions of the Late Quaternary hydrographic and atmospheric variability in the ITF region were mainly based on clay mineral assemblages, stable isotope compositions ($\delta^{18}O$, $\delta^{13}C$) of planktonic and benthic foraminifera, as well as Mg/Ca thermometry (e.g., Gingele et al., 2001, 2002; Holbourn et al., 2005, 2011; Spooner et al., 2005; Xu et al., 2008; Zuraida et al., 2009).

This study focuses on marine isotope stage 3 (MIS3), which was characterized by rapid, millennial-scale climate variability, i.e., Dansgaard–Oschger interstadials and Heinrich stadials. Although these climate oscillations were most pronounced in higher latitudes of the northern hemisphere, they have also been observed in subtropical and tropical regions, as well as in the southern hemisphere (Voelker et al., 2002; Lynch-Stieglitz, 2004; Huber et al., 2006; Piotrowski et al., 2008). In addition, this period of time was characterized by significant sea level changes ranging from 40 to 100 m below the present level (Siddall et al., 2003), which would have resulted in exposure of large parts of the shelf of the Indonesian Archipelago, and significantly affected ITF current pathways (in analogy to the sea level changes during the LGM; De Deckker et al., 2002).

Based on analyses of foraminiferal assemblages and stable isotopes ($\delta^{18}O$, $\delta^{13}C$), a generally drier climate over the Indonesian Archipelago has been suggested for MIS3 due to the ITCZ being permanently located to the north of the Banda Sea (Spooner et al., 2005). In analogy to modern observations, this atmospheric setup would have resulted in constant 'SE monsoon'-like conditions accompanied by a thinner mixed layer and an intensified throughflow. On shorter millennial to centennial time-scales within MIS3, the variability of the ITF intensity has been found to respond to variations in global oceanic circulation, sea level changes, as well as orbitally driven monsoon fluctuations (Holbourn et al., 2005; Dürkop et al., 2008; Zuraida et al., 2009; these authors used sediments of core MD01-2378 as well). According to these studies lower sea levels during stadial periods (i.e., Heinrich events) were associated with slowdowns of the ITF.

This study aims to investigate past environmental changes within the western ITF and their controlling factors focussing on marine isotope stage 3 (MIS3). We combine the evidence provided by independent approaches of analysing radiogenic isotope compositions (i.e., neodymium, strontium, lead) of the detrital clay size

fraction and the authigenic seawater derived fractions of the sediment to reconstruct changes in past water circulation and in climatically driven continental inputs.

2. Radiogenic isotope compositions of the ITF area

2.1. Paleoceanographic reconstructions

Radiogenic isotope compositions have become a widely used tool in paleoceanography to reconstruct changes of ocean circulation and water mass mixing, as well as of the variability in sediment provenance. The radiogenic isotope signatures of neodymium (Nd), lead (Pb), and strontium (Sr), have been extracted from various marine archives. Detrital clay minerals carry information about sediment provenance (e.g., Fagel et al., 2002, 2004; Grousset and Biscaye, 2005; Ehlert et al., 2011; Stumpf et al., 2011) while Fe–Mn crusts (e.g., Abouchami et al., 1999; Frank, 2002; Muiños et al., 2008) and Fe–Mn oxyhydroxide coatings of sediments (e.g., Gutjahr et al., 2008, 2009; Piotrowski et al., 2008; Stumpf et al., 2010), as well as deep-sea corals (e.g., Colin et al., 2010; Copard et al., 2010; van de Flierdt et al., 2010) and benthic foraminifera (e.g., Klevenz et al., 2008) have been used to reconstruct past bottom water circulation. In addition, Nd isotope compositions of surface and near surface water masses have been reconstructed from planktonic foraminiferal calcite in marine sediments (Vance and Burton, 1999; Burton and Vance, 2000; Vance et al., 2004; Stoll et al., 2007; Osborne et al., 2008, 2010; Pena et al., 2013). However, the use of planktonic foraminifera as an archive for past surface water signatures is complicated by contamination with incorporated clays, incomplete removal of early diagenetic Fe–Mn oxyhydroxide coatings, or by exchange processes with pore waters (Roberts et al., 2010; Tachikawa et al., 2013). Furthermore, it has been shown that the oxyhydroxide phases associated with deposited planktonic foraminifera can be used as reliable archive of past bottom water signatures (Charbonnier et al., 2012; Roberts et al., 2012; Kraft et al., 2013) challenging the reliability of earlier reconstructions of past surface water Nd isotope compositions.

For this study we analysed radiogenic isotope compositions of different fractions of the marine sediments (authigenic and detrital phases) in order to constrain reliable proxy data for past water mass mixing and erosional inputs into the easternmost Indian Ocean and to provide a paleoceanographic reconstruction of the Indonesian Throughflow and proximal seas during MIS3.

2.2. Dissolved radiogenic Nd isotope signatures

Although the Indonesian Throughflow has been the subject of numerous oceanographic studies within the last decades, dissolved Nd isotope data of regional water masses are sparse. Amakawa et al. (2000) compiled Nd isotopic compositions of surface waters of the Indonesian Seas (sampled during Austral summer between December and February 1996/97) and showed that western Pacific surface waters (εNd about −4) are strongly modified during their passage through the Indonesian Archipelago (to εNd > −1.5). Unfortunately, no data are available from the Banda Sea itself. However, Nd isotope signatures in the water column of the ITF outflow in the western Timor Sea show less radiogenic values of −3.9 < εNd < −4.6 suggesting intense mixing with Indian Ocean waters. To date, there is only one study by Jeandel et al. (1998) providing dissolved water column Nd isotope profiles within the area of the Timor Sea and the easternmost Indian Ocean (also sampled during Austral summer in February 1992; Sprintall et al., 2002). A profile upstream of this study's core location in the Timor Sea (st. 33; Figs. 1 and 2) documents Nd isotope compositions of intermediate waters between εNd = −4.1 (600 m) and εNd = −4.9 (1600 m). Nearby stations also show only minor stratification in terms of Nd isotope composition in surface and intermediate waters (signatures are close to εNd = −5; Figs. 1 and 2) and a change to less radiogenic values in deeper water masses. Bottom waters below 2500 m water depth shift to significantly less radiogenic εNd values between −6.0 and −7.3 and have been identified as Indian Ocean Bottom Water with negligible contributions from the Indonesian Throughflow (Jeandel et al., 1998).

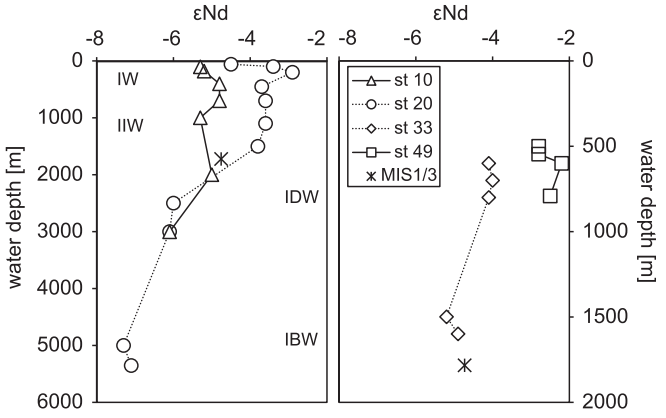

Fig. 2. εNd distribution in water column profiles from locations in the western Timor Sea (see Fig. 1; Jeandel et al., 1998; mind the different depth scales) compared with the averaged MIS1/3 Nd isotope data (extracted from planktonic foraminifera, Table 1) obtained from core MD01-2378 at 1783 m water depth. (IW = Indonesian Water, IIW = Indonesian Intermediate Water, IBW = Indian Bottom Water, IDW = Indian Deep Water).

2.3. Signatures of rocks and detrital sediments

The Indonesian Archipelago is a complex tectonic system, in which the Sunda and Banda Arcs collide with the Australian continental margin and which is driven by subduction of the Indian–Australian and New Guinea plates (e.g., Vroon et al., 1995; Ehlert et al., 2011; and references therein). Consequently, the islands of the Indonesian Archipelago mainly consist of younger volcanic island arc rocks of Cenozoic age. NW Australia, on the other hand, is characterized by much older lithologies comprising Archaean and Proterozoic cratonic rocks, as well as Palaeozoic sediment formations. Detailed analyses of clay mineral assemblages of marine surface sediments between Indonesia and NW Australia reflect these distinct source areas and provided the means for identification of three distinct terrestrial provenances: 'South Sumatra and Java', 'Timor', and 'NW Australia' (Gingele et al., 2001).

Due to the fact that radiogenic isotope compositions of rocks are a function of lithology and age, Indonesia and NW Australia contribute erosional products with vastly different isotope signatures via weathering driven eolian and riverine particle transport (e.g., Goldstein et al., 1984; Jeandel et al., 2007). The weathering products of the older lithologies of NW Australia typically carry less radiogenic Nd isotope signatures (−8 < εNd < −22; where $\varepsilon Nd = [(^{143}Nd/^{144}Nd)_{sample}/(^{143}Nd/^{144}Nd)_{CHUR} - 1] \times 10^4$, present day CHUR = 0.512638, Jacobsen and Wasserburg, 1980), and more radiogenic Sr and Pb isotope compositions ($0.73 < {}^{87}Sr/{}^{86}Sr < 0.83$; $18.6 < {}^{206}Pb/{}^{204}Pb < 19.9$; Vroon et al., 1995; Ehlert et al., 2011; Fig. 1). In contrast, the detrital material originating from the younger volcanics of the Indonesian region show more radiogenic Nd isotope compositions (+2 < εNd < −13), and less radiogenic signatures of Sr and Pb ($0.70 < {}^{87}Sr/{}^{86}Sr < 0.74$; $17.25 < {}^{206}Pb/{}^{204}Pb < 19.25$; Vroon et al., 1995; Ehlert et al., 2011; Fig. 1).

3. Material and methods

3.1. Core selection and age model

Sediment core MD01-2378 was recovered within the framework of the International Marine Global Change Study (IMAGES) on the NW Australian shelf margin (Scott Plateau, 13° 04.95′ S and 121° 47.27′ E, 1783 m water depth, Fig. 1) by RV Marion-Dufresne in 2001 (Bassinot et al., 2002). The core site is at a location where the Indonesian Throughflow ultimately enters the Indian Ocean in the western Timor Sea, and is thus well suited to trace changes in ITF intensity and dynamics through time. Analyses of stable oxygen and carbon isotopes, as well as radiocarbon dating indicate a complete recovery of a continuous and undisturbed sequence of hemipelagic sediments since marine isotope stage 12 (Holbourn et al., 2005). The age model for core MD01-2378 is based on radiocarbon dating on planktonic foraminifera and benthic oxygen isotope stratigraphy correlated to available ice core data (Dürkop et al., 2008, and supplementary material therein), and it is available via the PANGAEA database (www.pangaea.de, doi10.1594/PANGAEA.666556).

3.2. Carbonate fraction

Neodymium isotope compositions of differently processed batches of planktonic foraminiferal shells were analysed in order to determine the most efficient method to extract a reliable paleo surface water Nd isotope signature from the cleaned foraminiferal carbonate fraction of this sediment core. The methods varied in terms of foraminiferal species and size fraction, sample weight, and extraction/cleaning protocols. In addition, Mn/Ca element ratios of the sample solutions (batches 1–3) were monitored to assess the efficiency of removal of authigenic Fe–Mn oxyhydroxides. These parameters, as well as the cleaning methods applied to the four different test batches used in this study are described below (see also Table 1). Except the batch 1 samples, which did not undergo a pre-cleaning step, all hand-picked foraminiferal samples were cracked, rinsed and subjected to oxidative and reductive cleaning procedures to remove contaminant phases prior to sample dissolution and element purification.

3.2.1. Batch 1

An average of 5 mg (about 100 specimens) per sample (n = 10) of the planktonic species *Pulleniatina obliquiloculata* from the size fraction > 250 μm (three samples were taken from > 315 μm) were tested. The foraminiferal shells were dissolved applying a flow-through method developed by Haley and Klinkhammer (2002).

3.2.2. Batch 2

An average of 20 mg of bulk planktonic foraminifera (size fraction > 400 μm, n = 8) were subjected to a batch cleaning method (Boyle, 1981; Burton and Vance, 2000; Vance et al., 2004) adjusted following Kraft et al. (2013).

3.2.3. Batch 3

Repeated sample preparation as for batch 2 (bulk planktonic foraminifera, n = 8, batch cleaning method), but using the size fraction > 315 μm and an average sample weight of 30 mg.

3.2.4. Batch 4

An average of 40 mg of bulk planktonic foraminifera samples (n = 7) of the size fraction > 315 μm (one sample > 250 μm) were subjected to the batch cleaning method. These samples comprise a subset of the samples used for the analyses of the oxide (chapter 3.3) and detrital fractions (chapter 3.4).

Table 1
Compilation of Nd isotope data for all samples from the carbonate fraction, as well as elemental Mn/Ca ratios for a subset of the samples. The table is divided into the four batches of foraminifera used in this study. All samples are from IMAGES core MD01-2378 (13° 04.95′ S, 121° 47.27′ E, 1783 m water depth) recovered in 2001.

Tot. depth [cm]	PANGAEA age [cal ka B.P.]	Size fraction [μm]	spl weight [mg]	εNd	± εNd [2σ SE]	Mn/Ca [μmol/mol]
Batch 1 – mono species *Pulleniatina obliquiloculata*, flow-through cleaning method						
432.5	23.6	>315	n.a.	−4.17	±1.0	679.3
453.5	24.2	>250	4.72	−9.16	±2.0	550.5
527.5	28.9	>250	4.72	−5.19	±0.6	490.8
573.5	32.3	>250	4.72	−5.26	±0.6	753.2
647.5	38.6	>250	4.72	−4.53	±0.6	324.5
693.5	42.6	>250	4.72	−3.71	±0.6	587.7
737.5	46.8	>250	4.81	−4.81	±0.6	445.1
754.5	48.7	>250	5.00	−4.82	±0.6	842.9
813.5	55.1	>315	5.29	−4.25	±0.6	662.1
835.5	57.4	>315	4.91	−8.22	±1.0	907.9
Batch 2 – bulk planktonic foraminifera, batch cleaning method						
74.5	4.3	>400	20.3	−5.15	±0.5	184.2
98.5	5.5	>400	20.6	−5.58	±0.5	172.4
530.5	29.1	>400	20.2	−4.57	±0.6	209.9
544.5	30.0	>400	21.4	−4.92	±0.6	164.0
628.5	37.1	>400	21.3	−3.47	±0.5	136.2
657.5	39.4	>400	20.9	−4.21	±0.5	190.6
734.5	46.5	>400	20.0	−4.33	±0.5	186.6
743.5	47.5	>400	21.3	−4.50	±0.5	196.4
Batch 3 – bulk planktonic foraminifera, batch cleaning method						
74.5	4.3	>315	31.3	−5.33	±0.5	274.9
98.5	5.5	>315	29.7	−4.96	±0.5	222.2
530.5	29.1	>315	34.1	−4.53	±0.5	252.0
544.5	30.0	>315	29.7	−4.53	±0.5	223.5
628.5	37.1	>315	31.3	−4.36	±0.5	231.4
657.5	39.4	>315	27.4	−4.14	±0.5	201.8
734.5	46.5	>315	35.1	−4.80	±0.5	234.6
743.5	47.5	>315	27.9	−4.34	±0.5	268.6
Batch 4 – bulk planktonic foraminifera, batch cleaning method						
106.5	5.9	>315	37.1	−4.80	±0.6	n.a.
449.0	24.0	>315	36.9	−4.30	±0.6	n.a.
758.5	49.1	>315	42.1	−4.70	±0.6	n.a.
780.5	51.5	>315	36.6	−4.40	±0.6	n.a.
836.5	57.6	>315	41.7	−4.80	±0.6	n.a.
874.5	61.7	>315	38.5	−5.20	±0.6	n.a.
901.5	64.3	>250	36.6	−5.20	±0.6	n.a.

3.3. Oxide fraction

The 'oxide fraction' refers to the authigenic, early diagenetic ferromanganese oxyhydroxide coatings precipitating on particle surfaces within oxic and suboxic waters close to the sediment–water interface, which incorporate the ambient dissolved trace metal compositions (e.g., neodymium) of bottom waters (Rutberg et al., 2000; Bayon et al., 2002). The extraction of the Nd isotope composition of the bottom waters from the oxide fraction followed a previously published protocol (slightly modified from Gutjahr et al., 2007; Stumpf et al., 2010). The procedure consists of the sequential dissolution of the bulk sediment samples starting with removal of the carbonate fraction followed by weak reductive leaching of the oxide fraction in order to prevent potential contamination by partial dissolution of the detrital fraction of the sediment. A total of 20 samples of sediment core MD01-2378 (sample weight about 3 g of dry bulk sediment, Table 2) were processed in order to determine the Nd isotope composition of the oxide fraction representing the corresponding bottom water signature during the period of interest. Furthermore, aliquots of the samples (sample weight about 2 g of dry bulk sediment, Table 2) have been reductively leached using the same leaching protocol but without preceding carbonate removal, in order to assess potential procedural sample contamination of authigenic bottom water Nd isotope signatures by contributions from the carbonate fraction

Table 2
Nd, Sr, Pb isotope data from the oxide and detrital fractions for all samples. εNd values are reported for bulk leachates (BL), detrital leachates (DL) and dissolved clays (DC). Sr and Pb isotope data represent dissolved clays only. Values in squared brackets represent 2σ standard errors for the respective isotope measurements. All samples are from IMAGES core MD01-2378 (13° 04.95′ S, 121° 47.27′ E, 1783 m water depth) recovered in 2001.

Tot. depth [cm]	PANGAEA age [cal ka B.P.]	εNd, BL[a] [± 0.4]	εNd, DL[a] [± 0.4]	εNd, DC[a] [± 1.0]	$^{87}Sr/^{86}Sr$ [± 0.00002]	$^{208}Pb/^{204}Pb$ [± 0.014]	$^{207}Pb/^{204}Pb$ [± 0.066]	$^{206}Pb/^{204}Pb$ [± 0.036]	$^{208}Pb/^{206}Pb$ [± 0.003]	$^{207}Pb/^{206}Pb$ [± 0.001]
432.5	23.6	−4.58	−4.88	−8.96	0.718949	39.0684	15.6865	18.8892	2.0685	0.8304
453	24.2	−4.60	−4.97	−8.80	0.719277	38.9525	15.6622	18.8259	2.0691	0.8319
527	28.8	−4.60	−4.99	−8.81	0.719192	39.1464	15.6965	18.9385	2.0670	0.8288
530	29.0	−4.73	−5.10	−8.77	0.719368	39.1416	15.6930	18.9351	2.0671	0.8287
544	29.9	−4.69	−5.03	−9.89	0.719501	39.1499	15.6924	18.9500	2.0659	0.8280
573	32.2	−4.90	−4.89	−8.23	0.720402	39.2488	15.7284	18.9958	2.0662	0.8279
628	37.0	−5.15	−5.13	−9.00	0.720045	39.1978	15.7039	18.9876	2.0642	0.8270
647	38.5	−4.93	−5.24	−8.98	0.719166	38.9995	15.6857	18.8661	2.0671	0.8314
657	39.3	−5.10	−5.06	−8.28	0.718255	39.1717	15.6980	18.9723	2.0646	0.8273
693	42.4	−4.91	−5.24	−8.22	0.720124	39.1735	15.6954	18.9785	2.0641	0.8269
734	46.4	−5.04	−5.40	−8.67	0.721168	39.1912	15.7054	18.9862	2.0640	0.8271
737	46.7	−5.18	−5.19	−8.33	0.721409	39.1747	15.6999	18.9767	2.0643	0.8273
743	47.4	−5.10	−5.05	−8.18	0.720898	39.2100	15.7053	19.0022	2.0634	0.8265
754	48.6	−5.06	−5.16	−9.21	0.721633	38.3698	15.6534	18.4794	2.0764	0.8470
758	49.0	−5.04	−4.98	−8.82	0.721293	38.4848	15.6594	18.5510	2.0746	0.8441
780	51.4	−5.02	−4.99	−11.24	0.721473	38.5133	15.6555	18.5708	2.0738	0.8430
813	55.0	−5.02	−5.00	−10.36	0.722121	38.8908	15.6791	18.8016	2.0685	0.8339
835	57.3	−5.10	−5.01	−9.85	0.721585	38.5836	15.6622	18.6157	2.0727	0.8413
874	61.6	−5.03	−4.82	−8.52	0.720361	38.7143	15.6698	18.6909	2.0713	0.8383
899.5	64.0	−5.17	−5.49	−8.12	0.722165	38.3559	15.6474	18.4733	2.0764	0.8470

[a] BL = bulk leachates: DL = detrital leachates; DC = dissolved clays; Sr and Pb data is available only for dissolved clays.

that are expected to reflect Nd from surface and subsurface water masses.

3.4. Detrital fraction

The residual fraction of the decarbonated and reductively leached samples was subjected to a mixture of hydrogen peroxide/acetic acid in an ultrasonic bath to eliminate residual oxides and organic matter. From the cleaned bulk detrital sediment, the clay fraction (<2 μm) was separated using a centrifuge-based Atterberg method. The detrital clay fraction (about 30 mg of dry sample, Table 2) was completely digested in a mixture of concentrated $HF–HNO_3–HClO_4$ on a hotplate. The dissolved samples were then subjected to standard element purification procedures for neodymium, strontium, and lead as described below. The Nd, Sr, Pb isotope compositions of the detrital fraction were employed as a provenance tracer to identify potential changes of the source areas supplying erosional material to the core location through time. For detailed reference to the separation and chemical treatment of the clay fraction see Stumpf et al. (2011, and references therein).

3.5. Element purification and analyses of radiogenic isotope compositions

The Nd in all carbonate fraction samples was purified using a large volume Eichrom® Ln-spec resin bed (3.14 ml, 50–100 μm) in a single-step ion chromatographic procedure (Kraft et al., 2013). Separation and purification of Nd contained in the oxide and detrital fractions followed standard two-step chromatographic procedures published by Cohen et al. (1988), Barrat et al. (1996), and Le Fèvre and Pin (2005). Further, the Pb and Sr from within the detrital fraction was purified using the standard two-step protocols published by Galer and O'Nions (1989), and Lugmair and Galer (1992) for Pb, and Horwitz et al. (1992) and Bayon et al. (2002) for Sr. For a more detailed description of the applied chromatographic methods see Stumpf et al. (2010) for reference.

All isotope measurements were carried out on a *Nu instruments* MC-ICP-MS at GEOMAR, Kiel. Due to the low Nd concentrations in the carbonate fractions, these samples were run in manual time resolved mode, while all other samples were measured in automated mode using an autosampler. Measured neodymium isotope ratios ($^{143}Nd/^{144}Nd$) were mass bias corrected to $^{146}Nd/^{144}Nd = 0.7219$ and normalized to the accepted value of JNdi-1 standard of 0.512115 (Tanaka et al., 2000). Radiogenic $^{87}Sr/^{86}Sr$ ratios were corrected for isobaric interferences (^{86}Kr, ^{87}Rb) and for mass bias using $^{86}Sr/^{88}Sr = 0.1194$ (Steiger and Jäger, 1977) prior to standard normalization to the accepted value for NBS987 ($^{87}Sr/^{86}Sr = 0.710245$). All reported Pb isotope data were determined using a standard-sample bracketing method (Albarède et al., 2004) and were normalized to the accepted values of Pb standard NBS981 (Abouchami et al., 1999). Repeated measurements of standards were used to evaluate the reproducibility of the isotope measurements (Tables 1 and 2), blank levels for all three isotope systems were considered negligible.

4. Results

4.1. Carbonate fraction

In order to reliably determine the authigenic paleo surface/subsurface Nd isotope compositions from the foraminiferal carbonate, we subjected four different batches of planktonic foraminifera (monospecific and bulk planktonic) to variable extraction procedures (Table 1). Of the four processed batches of the carbonate fraction, 'batch 1' displays the largest range of Nd isotope compositions (εNd = −3.7 < to −5.3; Fig. 3) but is also characterized by the highest analytical uncertainties. Moreover, this 'batch 1' contained two data outliers at εNd = −9.2 and −8.2 that most likely originate from contamination with detrital clay signatures, given that these two values are in good agreement with the Nd isotope signatures of the clay-size detrital fraction of the same samples (Fig. 3). 'Batch 2' and 'batch 3' show a slightly smaller range of Nd isotope compositions (εNd = −3.5 < to −4.9; Fig. 3), but considering that 'batch 3' represents repeats of 'batch 2' samples they are supposed to replicate the exact same Nd isotope signatures. After averaging the values of these two treatments, the εNd signatures of the MIS3 record are invariable within analytical precision (±0.5 εNd units, Table 1). Likewise, the εNd signatures of 'batch 4' are uniform within analytical error.

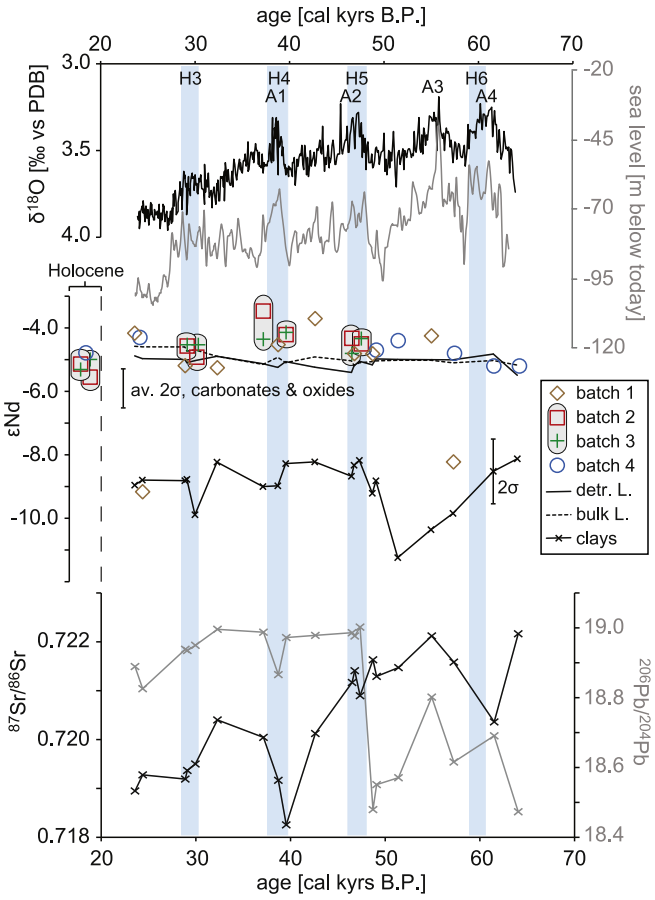

Fig. 3. Time series of all parameters determined in core MD01-2378 for MIS3. Top: $\delta^{18}O$ record of benthic foraminifera (Dürkop et al., 2008), and sea level curve from the central Red Sea (Siddall et al., 2003) tuned to MD01-2378 to maintain chronological consistency with GICC05 timescale (Svensson et al., 2006). Vertical bars highlight occurrence and duration of four Heinrich events (H3–H6), A1–A4 refer to Antarctic warm events during MIS3 (Dürkop et al., 2008; Zuraida et al., 2009). Centre: εNd records of the four different test batches of the carbonate fraction (single symbols; shaded circles highlight measurements of sample repeats of batches 2 and 3) and the two oxide fraction time series (lines without symbols; solid line: detrital leachates, dashed line: bulk leachates), as well as the clay-size detrital fraction Nd isotope data on the same axis (lines with data point symbols). Please note that MIS1 εNd values are not plotted against age, for correct ages refer to Table 1. Bottom: $^{87}Sr/^{86}Sr$ and $^{206}Pb/^{204}Pb$ records of the clay-size detrital fraction. Representative error bars for εNd values are given for the respective records. $^{206}Pb/^{204}Pb$ errors are about symbol size, $^{87}Sr/^{86}Sr$ errors are smaller than symbol size. All analytical errors (2σ) of the radiogenic isotope compositions are reported in Tables 1 and 2.

In summary, no significant variability of the seawater Nd isotope compositions was documented by the carbonate fraction of core MD01-2378 during MIS3. The average εNd value for all samples (n = 28) of the carbonate fraction is −4.5(±0.6). Despite the overall coarse temporal resolution of the record, the occurrence of short-term millennial to centennial changes can be excluded because some high resolution sections that were selected based on rapid transitions in the oxygen isotope record between 48 and 46 ka, as well as around 39 and 30 ka (Dürkop et al., 2008) did also not show any significant Nd isotope changes. Furthermore, a total of five MIS1 samples of core MD01-2378 have been processed within batches 2–4 (Table 1) with an average εNd = −5.1(±0.5) barley showing a significant variation from the MIS3 Nd isotope signatures as well.

4.2. Oxide fraction

The ferromanganese oxide coatings of the decarbonated detrital sediment were used to determine the Nd isotope compositions of the bottom waters at the location of MD01-2378 during MIS3. In order to assess potential biases of the Nd isotope signatures originating from removal of the carbonate fraction, samples of the bulk marine sediment were processed for comparison. As can be seen in Fig. 3, the resulting two records of the oxide fraction (detrital leachates and bulk leachates) document essentially the same uniform values near εNd = −5.0 (±0.4; n = 40, Table 2) throughout the entire MIS3. Due to the similarity of the two differently obtained records, no contamination of the extracted bottom water Nd isotope signatures originating from the carbonate fraction is detectable at our study site.

4.3. Detrital fraction

The εNd signatures of the clay-size detrital fraction range from −8.1 to −11.2 (Fig. 3). The record shows a distinct trend to less radiogenic εNd values in the early part of MIS3 (64–51 ka) followed by a return to εNd = −9 (at about 49 ka). For the rest of MIS3, the detrital Nd isotope signatures were close to εNd = −9.

The radiogenic Sr and Pb isotope signatures of the clay-size detrital fraction document significant shifts towards less radiogenic Sr isotope ratios and more radiogenic Pb isotope compositions, respectively, during MIS3 (Fig. 3). Accordingly, the records can be divided into an older and a younger phase of MIS3. The older part from 64 ka to 47–49 ka was overall characterized by more radiogenic Sr and less radiogenic Pb isotope signatures ($^{206}Pb/^{204}Pb$), while the remaining younger part of MIS3 showed pronouncedly less radiogenic Sr and more radiogenic Pb isotope ratios. It is noted that the subdivision of the records is more distinctive for the Pb isotope compositions, while the Sr isotope record arguably shows a more gradual shift to less radiogenic values over time. Interestingly, the timing of this transition is different with respect to the two isotope systems. While the radiogenic Sr isotope record shows the most pronounced change between 46.4 and 40 ka, the transition of the Pb isotope record occurred sharply between 48.6 and 47.4 ka, thus slightly postdating the main shift in Nd isotope signatures. Given that all detrital radiogenic isotope compositions were measured on the same sample solutions, the difference in timing cannot be caused by sampling or dating uncertainties of the records but must originate from provenance changes of the material.

5. Discussion

5.1. MIS3 seawater Nd isotope compositions

5.1.1. Carbonate fraction

All four applied methods to extract surface/subsurface seawater Nd isotope compositions from planktonic foraminifera produced essentially the same εNd values, which are also consistent with the present day distribution of dissolved Nd isotope compositions in the western Timor Sea (Figs. 1 and 2). In surface and subsurface waters near the MD01-2378 core site, Jeandel et al. (1998) and Amakawa et al. (2000) found εNd signatures between −3.9 and −5.2, which is in very good agreement with the data measured on the foraminifera (MIS1/3). Unfortunately, present day Nd isotope compositions in the western Timor Sea are invariant within the upper 2000 m and only show a change to less radiogenic signatures below that depth (Jeandel et al., 1998). Based on these data we thus cannot unambiguously distinguish if the cleaned planktonic foraminifera samples from our core located at 1783 m water depth acquired their Nd isotopic signature from surface/subsurface waters or from exchange processes with bottom waters after deposition (e.g. Roberts et al., 2010, 2012). The latter is supported by high Mn/Ca ratios of 136–908 μmol/mol measured on the

sample solutions of 'batches 1–3' (Table 1). The elevated Mn/Ca ratios, in combination with the uniform bottom water Nd signatures (obtained from the oxide fraction) thus suggest incomplete removal of the Fe–Mn oxyhydroxides from the planktonic foraminiferal tests and the Nd isotope compositions obtained from the carbonate fraction are likely to mainly represent past bottom water signatures instead of surface/subsurface water compositions (Roberts et al., 2010, 2012; Kraft et al., 2013).

5.1.2. Oxide fraction

At present, the core site at 1783 m water depth is located within the lower part of Indonesian Intermediate Water (IIW; $-3.8 < \varepsilon Nd < -5.2$, Fig. 2), close to the transition to Indian Deep Water (IDW; $\varepsilon Nd < -6.1$; Jeandel et al., 1998). Considering the consistent paleo bottom water records of the oxide fraction with values near $\varepsilon Nd = -5.0$, which is in excellent agreement with today's bottom water signature, we deduce that the intermediate to deep water structure of the water column in the western Timor Sea remained constant throughout MIS3, and thus was not affected by any potential changes in ITF intensity in the water layers above.

However, the Nd isotope compositions of the oxide fraction show a small offset of about 0.5 εNd units (although statistically barely significant regarding the reported errors) to less radiogenic Nd isotope compositions obtained from the carbonate fraction for almost the entire MIS3 (Fig. 3). Assuming that this small offset between the two records is real, it would suggest contributions from surface/subsurface waters with more radiogenic Nd isotope signatures to the location of our core site. Since such more radiogenic Nd signatures are only found within the Indonesian Seas, the consistent offset would point to a persistently strong ITF during entire MIS3. However, since we cannot unambiguously tell if surface/subsurface water Nd signatures were reliably extracted, any conclusions on hydrographic fluctuations of the ITF during MIS3 based on our Nd isotope records must remain speculative.

5.2. Changes in sediment provenance during MIS3

The radiogenic Nd, Sr, and Pb isotope compositions of the clay-size detrital fraction serve to constrain changes in the provenance of the terrigenous sediment fraction of core MD01-2378, i.e., the Indonesian Archipelago versus NW Australia (Fig. 4).

The εNd signature of the detrital fraction ranges from −8.1 to −11.2 with an average value of $\varepsilon Nd = -9$ (Fig. 3, Table 2), which is significantly less radiogenic then the extracted corresponding bottom water values and which is in good agreement with Nd isotope compositions of the clay fraction in a core at a location close to MD01-2378 for the same period of time (Ehlert et al., 2011; the sampling resolution in the latter study was, however, very coarse and comprised only four samples within MIS3). The radiogenic Sr isotope compositions of the clay fraction range from 0.718 to 0.722, while the $^{206}Pb/^{204}Pb$ ratios range from about 18.47 to 19.0 (Fig. 3, Table 2). While both the radiogenic Sr and Pb isotope compositions are in the same range as the MIS3 records published by Ehlert et al. (2011), the absolute values are offset: $^{87}Sr/^{86}Sr$ ratios tend to be more radiogenic and show barely any variation over time, while the $^{206}Pb/^{204}Pb$ record on average shows less radiogenic values compared to core MD01-2378, and documents almost an inversed pattern during MIS3. Given that both the radiogenic Sr and Pb isotope compositions are affected by grain-size fractionation during weathering and transport of the sediments, these small differences in isotope ratios between the two records of the two cores may be the result of a slightly variable grain-size distribution within the analysed fine fraction of the sediment samples. However, the Ehlert et al. (2011) core is located at 2452 m depth (~700 m deeper than MD01-2378 on the nearby Scott plateau) and about 1°S closer to the NW Australian coast, and is thus likely to have received higher contributions from this supply area. Unfortunately, the interval of the most pronounced variabilities in our MIS3 isotope records prior to ~47 ka has not been sampled in the study by Ehlert et al. (2011).

The three radiogenic isotope records of core MD01-2378 show a pronounced variability during early MIS3 (prior to 47 ka), most likely related to sea level changes (Fig. 3). According to Siddall et al. (2003), the early phase of MIS3 experienced major global sea level fluctuations starting with a marked rise from −92 m to −39 m (61.4–54.8 ka), followed by a rapid regression back to −97 m at 49.2 ka. For the remaining MIS3, sea level fluctuated around an average value of −80 m with respect to today. These sea level fluctuations during early MIS3 significantly altered the coastlines, in particular in the shallow shelf regions (Fig. 1), and thus impacted hydrographic pathways and continental inputs due to changes in exposure/flooding of the large shelf areas (De Deckker et al., 2002). Interestingly, the Nd, Sr, and Pb isotope records each display a slightly different timing regarding the rapid regression between about 52.7 and 48.2 ka. The Nd isotope composition shifted first at 51.4–49.0 ka, followed by the radiogenic Pb isotope data at 48.6–47.4 ka, and finally, though certainly less abrupt than the Pb isotopes, the $^{87}Sr/^{86}Sr$ ratios changed to less radiogenic isotope compositions for samples younger than 46.4 ka. Given that the radiogenic isotope compositions of Nd, Pb, and Sr of the detrital fraction were purified and analysed from the same sample digestions, the different timings of these major changes are real. We suggest this observation to be caused by stepwise short-term changes in provenance during this period of time (most likely due to the changing sea level), which are, however, not unambiguously attributable to particular source areas due to lack of detailed information on the radiogenic isotope composition of the potential source areas, as well as the temporal resolution of our study.

In order to reconstruct changes in the provenance of the sediment, and to better understand the major variations during MIS3, the records of core MD01-2378 are compared to previously published radiogenic isotope compositions of surface sediments of the Indonesian Archipelago and NW Australia, as well as of detrital clay-size fractions of core top sediments along the ITF pathway (Fig. 4; modified from Vroon et al., 1995; Ehlert et al., 2011). Importantly, the clay-size detrital fraction of core MD01-2378, although deposited on the outer NW Australian shelf, has radiogenic isotope characteristics that suggest a main origin from within the Indonesian Archipelago, and only small contributions from the Australian continent throughout MIS3 (Fig. 4), which is fully consistent with a persistently strong ITF during MIS3. This observation is in agreement with a provenance analysis based on clay mineral assemblages that associated the location of core MD01-2378 with sediments from the Banda and Timor Seas, while a NW Australian provenance can only be found further to the west of our core location (Gingele et al., 2001). Alongi et al. (2013) suggested that the fine fraction of the marine sediment deposited in the Timor Trough is transported from as far upstream the Indonesian Throughflow as the Makassar Strait. It has also been shown that the suspended particle load of Australian rivers does not contribute sufficient amounts of clay-sized material to the Timor Sea to significantly overprint the radiogenic isotope signature originating from upstream the ITF pathway (Ehlert et al., 2011). Thus, variations in the radiogenic Nd, Sr, and Pb isotope records of core MD01-2378 were most likely a consequence of changing contributions to the suspended particle load within the ITF pathway rather than mixing of Indonesian and Australian sources.

As discussed above, the MIS3 isotope records can be divided into an older variable and a younger less variable phase, which appear to be related to sea level fluctuations, and which document mixing

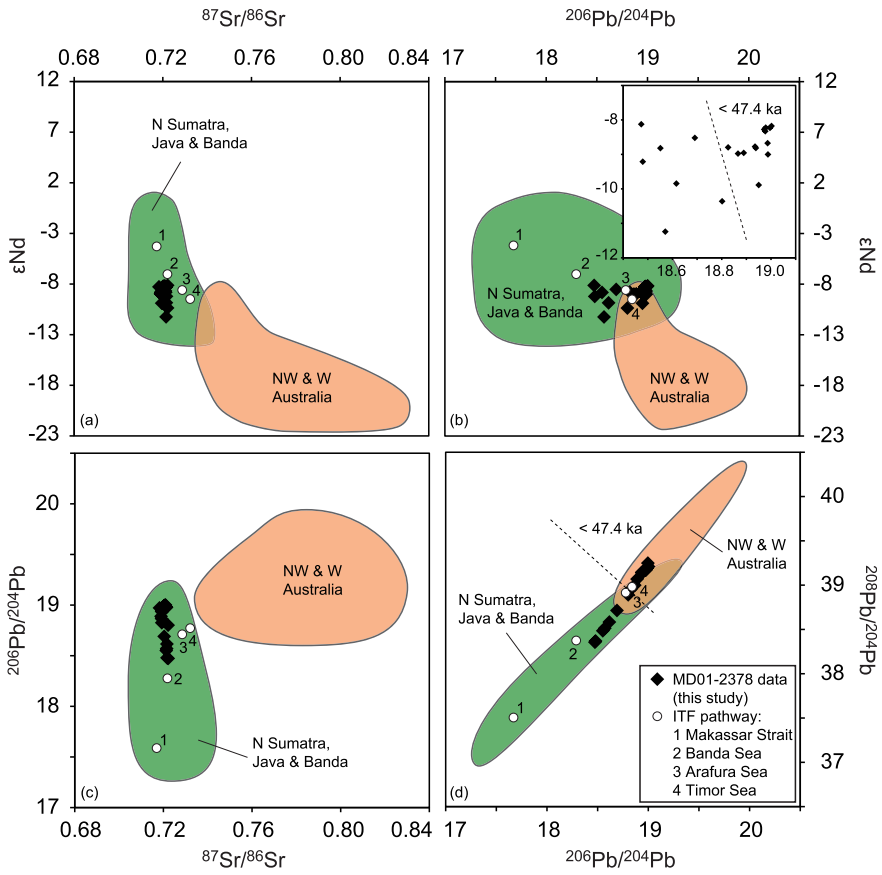

Fig. 4. Radiogenic Nd, Sr, Pb isotope compositions of the clay-size detrital fraction compared with potential endmember signatures obtained from the surface sediment fine fraction (modified from Ehlert et al., 2011): a) $^{87}Sr/^{86}Sr$ vs. εNd, b) $^{206}Pb/^{204}Pb$ vs. εNd, c) $^{87}Sr/^{86}Sr$ vs. $^{206}Pb/^{204}Pb$ and d) $^{206}Pb/^{204}Pb$ vs. $^{208}Pb/^{204}Pb$. The inset graph in (b) shows the data of this study at an expanded scale, the dashed lines in (b) and (d) separate the Pb isotope data into two arrays of different age. Open circles (numbers 1–4) refer to the clay-size fraction of marine core top sediments within the ITF pathway (Ehlert et al., 2011; Fig. 1).

within the Indonesian Archipelago. At present day, isotope compositions of detrital surface sediment fine fractions are roughly distributed along a mixing line within the ITF pathway (numbers 1–4 in Figs. 1 and 4, Ehlert et al., 2011). In analogy to this observation, the compositions of our younger MIS3 samples are closer to values characteristic for the Arafura and Timor Seas (numbers 3–4) while the older MIS3 samples seem to have been dominated by more distal sources such as the Makassar Strait and the Banda Sea (numbers 1–2). Because more energy is needed to transport suspended particles over longer distances, we argue that during the older part of MIS3, characterized by elevated sea levels and high amplitude fluctuations, the ITF was slightly intensified due to the enhanced contributions from more distal sediment sources compared to the younger phase of MIS3 with consistent sea level low stands and more proximal sediment provenance. This scenario is in agreement with a previous study on this core based on stable carbon and oxygen isotope compositions and Mg/Ca records (Zuraida et al., 2009). The results of our study do, however, not agree with a clay mineral study of a core located in the South Java Current which documented a slightly reduced intensity of the ITF in the early MIS3 until about 55 ka ago (Gingele et al., 2002), which may have been related to regional differences in current speed and origin of the currents between the two sites.

Furthermore, and in analogy to the present day Indo-Australian monsoon system, an intensified ITF corresponds to westwards blowing winds of the SE monsoon during Austral winter (March–September) with the ITCZ located at 10–15°N (Wijffels et al., 1996). Thus, we suggest permanent 'SE monsoon'-like conditions during MIS3, which is in agreement with a previous study published by Spooner et al. (2005).

6. Conclusions

The scope of this study is the investigation of intensity changes of the Indonesian Throughflow, as well as a reconstruction of the sedimentary depositional environment in the western Timor Sea during MIS3. For the first time, radiogenic isotope compositions of neodymium extracted from different sediment fractions of core MD01-2378, in combination with the radiogenic Nd, Sr, and Pb isotope compositions of the clay-size detrital fraction of the same sediment samples, have been used to obtain information on paleo circulation and to reconstruct changes in climatically driven sediment provenance of the detrital marine sediments in this area.

Although the applied extraction methods clearly provide paleo seawater data, it was not possible to distinguish surface/subsurface water Nd isotope signatures unequivocally from bottom water compositions, which is a consequence of the absence of water column stratification in terms of Nd isotope compositions combined with incomplete cleaning of the foraminiferal tests. The constant bottom water records suggest an essentially invariable intermediate to deep water structure and indicate that the mixture of water masses within the ITF remained essentially unchanged in the western Timor Sea during MIS3. A small but consistent offset of 0.5 εNd-units to more radiogenic Nd isotope compositions in the carbonate fraction compared to the oxide fraction may further support a persistently strong ITF (if it is assumed that the

foraminiferal carbonate fraction did at least partly preserve near surface water compositions), because more radiogenic Nd isotope compositions can only be found upstream the ITF within the Indonesian Seas. Further studies following a similar approach are necessary to support this conclusion from other locations within the ITF pathway and water depth, preferably with a more distinct water column stratification in terms of radiogenic Nd isotope compositions.

The provenance analyses based on the radiogenic Nd, Sr, and Pb isotope compositions of the clay-size detrital fraction suggest particle sources within the Indonesian Archipelago along the ITF pathway as main provenance for the fine fraction of the sediments deposited on the NW Australian shelf, which also argues for an overall strong ITF during MIS3. The variations in the isotope compositions of the clay fractions further suggest changing dynamics in particle transport within the ITF associated with sea level fluctuations, shelf sediment remobilization and variable flowpaths within the Indonesian Archipelago, and thus variability in ITF intensity, which cannot be resolved from the paleo seawater Nd isotope data, most likely because the isotopic signature of the different water masses was too similar. Accordingly, elevated sea levels and pronounced fluctuations recorded for the early MIS3 until about 47.4 ka ago promoted an intensified ITF while generally low sea levels during the remaining period of MIS3 suggest a less intense ITF thereafter.

Acknowledgements

This project was funded by the German Science Foundation (DFG), project Ku 649/25-1,2. We thank D. Nürnberg and A. Dürkop for discussions and proxy data for comparison, as well as for the stratigraphy of core MD01-2378.

References

Abouchami, W., Galer, S.J.G., Koschinski, A., 1999. Pb and Nd isotopes in NE Atlantic Fe-Mn crusts: proxies for trace metal paleosources and paleocean circulation. Geochim. Cosmochim. Acta 63 (10), 1489–1505.

Albarède, F., Telouk, P., Blichert-Toft, J., Boyet, M., Agranier, A., Nelson, B., 2004. Precise and accurate isotopic measurements using multiple-collector ICPMS. Geochim. Cosmochim. Acta 68 (12), 2725–2744.

Alongi, D.M., da Silva, M., Wasson, R.J., Wirasantosa, S., 2013. Sediment discharge and export of fluvial carbon and nutrients into the Arafura and Timor Seas: a regional synthesis. Mar. Geol. 343, 146–158.

Amakawa, H., Sotto Alibo, D., Nozaki, Y., 2000. Nd isotopic composition and REE pattern in the surface waters of the eastern Indian Ocean and its adjacent seas. Geochim. Cosmochim. Acta 64 (10), 1715–1727.

Barrat, J.A., Keller, F., Amossé, J., 1996. Determination of rare earth elements in sixteen silicate reference samples by ICP-MS after Tm addition and ion exchange separation. Geostand. Newsl. 20, 133–139.

Bassinot, F.C., Waelbroeck, C., Shipboard Scientific Party, 2002. IMAGES VII Cruise Report. Les Publications de l'Institut Français pour la Recherche et la Technologie Polaires. Les rapports de campagnes à la mer, 01, 435 pp.

Bayon, G., German, C.R., Boella, R.M., Milton, J.A., Taylor, R.N., Nesbitt, R.W., 2002. An improved method for extracting marine sediment fractions and its application to Sr and Nd isotopic analysis. Chem. Geol. 187, 179–199.

Boyle, E.A., 1981. Cadmium, zinc, copper, and barium in foraminifera tests. Earth Planet. Sci. Lett. 53, 11–35.

Burton, K.W., Vance, D., 2000. Glacial-interglacial variations in the neodymium isotope composition of seawater in the Bay of Bengal recorded by planktonic foraminifera. Earth Planet. Sci. Lett. 176, 425–441.

Charbonnier, G., Pucéat, E., Bayon, G., Desmares, D., Dera, G., Durlet, C., Deconinck, J.-F., Amédro, F., Gorlan, A.T., Pellenard, P., Bamou, B., 2012. Reconstruction of the Nd isotope composition of seawater on epicontinental seas: testing the potential of Fe-Mn oxyhydroxide coatings on foraminifera tests for deep-time investigations. Geochim. Cosmochim. Acta 99, 39–56.

Cohen, A.S., O'Nions, R.K., Siegenthaler, R., Griffin, W.L., 1988. Chronology of the pressure-temperature history recorded by a granulite terrain. Contrib. Mineral. Petrol. 98, 303–311.

Colin, C., Frank, N., Copard, K., Douville, E., 2010. Neodymium isotopic composition of deep-sea corals from the NE Atlantic: implications for past hydrological changes during the Holocene. Quat. Sci. Rev. 29, 2509–2517.

Copard, K., Colin, C., Douville, E., Freiwald, A., Gudmundsson, G., De Mol, B., Frank, N., 2010. Nd isotopes in deep-sea corals in the North-eastern Atlantic. Quat. Sci. Rev. 29, 2499–2508. http://dx.doi.org/10.1016/j.quascirev.2010.05.025.

De Deckker, P., Tapper, N.J., van der Kaars, S., 2002. The status of the Indo-Pacific Warm Pool and adjacent land at the Last Glacial Maximum. Glob. Planet. Change 35, 25–35.

Dürkop, A., Holbourn, A., Kuhnt, W., Zuraida, R., Andersen, N., Grootes, P.M., 2008. Centennial-scale climate variability in the Timor Sea during Marine Isotope Stage 3. Mar. Micropaleontol. 66, 208–221.

Ehlert, C., Frank, M., Haley, B.A., Böninger, U., De Deckker, P., Gingele, X., 2011. Current transport versus continental inputs in the eastern Indian Ocean: radiogenic isotope signatures of clay size sediments. Geochem. Geophys. Geosyst. 12, Q06017. http://dx.doi.org/10.1029/2011GC003544.

Fagel, N., Innocent, C., Gariepy, C., Hillaire-Marcel, C., 2002. Sources of Labrador Sea sediments since the last glacial maximum inferred from Nd-Pb isotopes. Geochim. Cosmochim. Acta 66 (14), 2569–2581.

Fagel, N., Hillaire-Marcel, C., Humblet, M., Brasseur, R., Weis, D., Stevenson, R., 2004. Nd and Pb isotope signatures of the clay-size fraction of Labrador Sea sediments during the Holocene: implications for the inception of the modern deep circulation pattern. Paleoceanography 19, PA3002. http://dx.doi.org/10.1029/2003PA000993.

Frank, M., 2002. Radiogenic isotopes: tracers of past ocean circulation and erosional input. Rev. Geophys. 40 (1), 1001. http://dx.doi.org/10.1029/2000RG000094.

Galer, S.J.G., O'Nions, R.K., 1989. Chemical and isotopic studies of ultramafic inclusions from the San Carlos volcanic field, Arizona: a bearing on their petrogenesis. J. Petrol. 30 (4), 1033–1064.

Gingele, F.X., De Deckker, P., Hillenbrand, C.-D., 2001. Clay mineral distribution in surface sediments between Indonesia and NW Australia – source and transport by ocean currents. Mar. Geol. 179, 135–146.

Gingele, F.X., De Deckker, P., Girault, A., Guichard, F., 2002. History of the South Java Current over the past 80 ka. Palaeogeogr. Palaeoclimatol. Palaeoecol. 183, 247–260.

Godfrey, J.S., 1996. The effect of the Indonesian throughflow on ocean circulation and heat exchange with the atmosphere: a review. J. Geophys. Res. 101 (C5), 12217–12237.

Goldstein, S.L., O'Nions, R.K., Hamilton, P.J., 1984. A Sm-Nd isotopic study of atmospheric dusts and particulates from major river systems. Earth Planet. Sci. Lett. 70, 221–236.

Gordon, A.L., 2005. Oceanography of the Indonesian seas and their throughflows. Oceanography 18 (4), 14–27.

Grousset, F.E., Biscaye, P.E., 2005. Tracing dust sources and transport patterns using Sr, Nd and Pb isotopes. Chem. Geol. 222, 149–167.

Gutjahr, M., Frank, M., Stirling, C.H., Klemm, V., van de Flierdt, T., Halliday, A.N., 2007. Reliable extraction of a deepwater trace metal isotope signal from Fe-Mn oxyhydroxide coatings of marine sediments. Chem. Geol. 242, 351–370.

Gutjahr, M., Frank, M., Stirling, C.H., Keigwin, L.D., Halliday, A.N., 2008. Tracing the Nd isotope evolution of North Atlantic deep and intermediate waters in the western North Atlantic since the Last Glacial Maximum from Blake Ridge sediments. Earth Planet. Sci. Lett. 266, 61–77.

Gutjahr, M., Frank, M., Halliday, A.N., Keigwin, L.D., 2009. Retreat of the Laurentide ice sheet tracked by the isotopic composition of Pb in western North Atlantic seawater during termination 1. Earth Planet. Sci. Lett. 286, 546–555.

Haley, B.A., Klinkhammer, G.P., 2002. Development of a flow-through system for cleaning and dissolving foraminiferal tests. Chem. Geol. 185, 51–69.

Hautala, S.L., Reid, J.L., Bray, N., 1996. The distribution and mixing of Pacific water masses in the Indonesian Seas. J. Geophys. Res. 101 (C5), 12375–12389.

Holbourn, A., Kuhnt, W., Kawamura, H., Jian, Z., Grootes, P., Erlenkeuser, H., Xu, J., 2005. Orbitally paced paleoproductivity variations in the Timor Sea and Indonesian Throughflow variability during the last 460 kyr. Paleoceanography 20, PA3002. http://dx.doi.org/10.1029/2004PA001094.

Holbourn, A., Kuhnt, W., Xu, J., 2011. Indonesian Throughflow variability during the last 140 ka: the Timor Sea outflow. Geological Society, London, Special Publications 355, pp. 283–303.

Horwitz, E.P., Chiarizia, R., Dietz, M.L., 1992. A novel strontium-selective extraction chromatographic resin. Solvent Extr. Ion Exch. 10 (2), 313–336.

Huber, C., Leuenberger, M., Spahni, R., Flückiger, J., Schwander, J., Stocker, T.F., Johnson, S., Landais, A., Jouzel, J., 2006. Isotope calibrated Greenland temperature record over Marine Isotope Stage 3 and its relation to CH_4. Earth Planet. Sci. Lett. 243, 504–519. http://dx.doi.org/10.1016/j.epsl.2006.01.002.

Jacobsen, S.B., Wasserburg, G.J., 1980. Sm-Nd isotopic evolution of chondrites. Earth Planet. Sci. Lett. 50, 139–155.

Jeandel, C., Thouron, D., Fieux, M., 1998. Concentrations and isotopic compositions of neodymium in the eastern Indian Ocean and Indonesian straits. Geochim. Cosmochim. Acta 62 (15), 2597–2607.

Jeandel, C., Arsouze, T., Lacan, F., Téchine, P., Dutay, J.-C., 2007. Isotopic Nd compositions and concentrations of the lithogenic inputs into the ocean: a compilation, with an emphasis on the margins. Chem. Geol. 239, 156–164.

Klevenz, V., Vance, D., Schmidt, D.N., Mezger, K., 2008. Neodymium isotopes in benthic foraminifera: core-top systematics and a down-core record from the Neogene south Atlantic. Earth Planet. Sci. Lett. 265, 571–587. http://dx.doi.org/10.1016/j.epsl.2007.10.053.

Kraft, S., Frank, M., Hathorne, E., Weldeab, S., 2013. Assessment of seawater Nd isotope signatures extracted from foraminiferal shells and authigenic phases from Gulf of Guinea sediments. Geochim. Cosmochim. Acta 121, 414–435. http://dx.doi.org/10.1016/j.gca.2013.07.029.

Le Fèvre, B., Pin, C., 2005. A straightforward separation scheme for concomitant Lu-Hf and Sm-Nd isotope ratio and isotope dilution analysis. Anal. Chim. Acta 543, 209–221.
Lugmair, G.W., Galer, S.J.G., 1992. Age and isotopic relationships among the angrites Lewis Cliff 86010 and Angra dos Reis. Geochim. Cosmochim. Acta 56, 1673–1694.
Lynch-Stieglitz, J., 2004. Hemispheric asynchrony of abrupt climate change. Science 304, 1919–1920. http://dx.doi.org/10.1126/science.1100374.
Muiños, S.B., Frank, M., Maden, C., Hein, J.R., van de Flierdt, T., Lebreiro, S.M., Gaspar, L., Monteiro, J.H., Halliday, A.N., 2008. New constraints on the Pb and Nd isotopic evolution of NE Atlantic water masses. Geochem. Geophys. Geosyst. 9 (2), Q02007. http://dx.doi.org/10.1029/2007GC001766.
Osborne, A.H., Vance, D., Rohling, E.J., Barton, N., Rogerson, M., Fello, N., 2008. A humid corridor across the Sahara for the migration of early modern humans out of Africa 120,000 years ago. Proc. Natl. Acad. Sci. 105 (43), 16444–16447. http://dx.doi.org/10.1073/pnas.0804472105.
Osborne, A.H., Marino, G., Vance, D., Rohling, E.J., 2010. Eastern Mediterranean surface water Nd during Eemian sapropel S5: monitoring northerly (mid-latitude) versus southerly (sub-tropical) freshwater contributions. Quat. Sci. Rev. 29, 2473–2483. http://dx.doi.org/10.1016/j.quascirev.2010.05.015.
Pena, L.D., Goldstein, S.L., Hemming, S.R., Jones, K.M., Calvo, E., Pelejero, C., Cacho, I., 2013. Rapid changes in meridional advection of southern ocean intermediate waters to the tropical Pacific during the last 30 kyr. Earth Planet. Sci. Lett. 368, 20–32. http://dx.doi.org/10.1016/j.epsl.2013.02.028.
Piotrowski, A.M., Goldstein, S.L., Hemming, S.R., Fairbanks, R.G., Zylberberg, D.R., 2008. Oscillating glacial northern and southern deep water formation from combined neodymium and carbon isotopes. Earth Planet. Sci. Lett. 272, 394–405. http://dx.doi.org/10.1016/j.epsl.2008.05.011.
Roberts, N.L., Piotrowski, A.M., McManus, J.F., Keigwin, L.D., 2010. Synchronous deglacial overturning and water mass source changes. Science 327 (75). http://dx.doi.org/10.1126/science.1178068.
Roberts, N.L., Piotrowski, A.M., Elderfield, H., Eglinton, T.I., Lomas, M.W., 2012. Rare earth element association with foraminifera. Geochim. Cosmochim. Acta 94, 57–71.
Rutberg, R.L., Hemming, S.R., Goldstein, S.L., 2000. Reduced North Atlantic Deep Water flux to the glacial Southern Ocean inferred from neodymium isotope ratios. Nature 405, 935–938.
Ruth, U., Bigler, M., Röthlisberger, R., Siggaard-Andersen, M.-L., Kipfstuhl, S., Goto-Azuma, K., Hansson, M.E., Johnsen, S.J., 2007. Ice core evidence for a very tight link between North Atlantic and east Asian glacial climate. Geophys. Res. Lett. 34, L03706. http://dx.doi.org/10.1029/2006GL027876.
Schmitz, W.J., 1995. On the interbasin-scale thermohaline circulation. Rev. Geophys. 33 (2), 151–173. http://dx.doi.org/10.1029/95RG00879.
Schott, F.A., Xie, S.-P., McCreary Jr., J.P., 2009. Indian ocean circulation and climate variabilty. Rev. Geophys. 47, 1–46. RG1002.
Siddall, M., Rohling, E.J., Almogi-Labin, A., Hemleben, Ch, Meischner, D., Schmelzer, I., Smeed, D.A., 2003. Sea-level fluctuations during the last glacial cycle. Nature 423, 853–858.
Spooner, M.I., Barrows, T.T., De Dekker, P., Paterne, M., 2005. Palaeoceanography of the Banda Sea, and Late Pleistocene initiation of the Northwest Monsoon. Glob. Planet. Change 49, 28–46. http://dx.doi.org/10.1016/j.gloplacha2005.05.002.
Sprintall, J., Wijffels, S., Chereskin, T., Bray, N., 2002. The JADE and WOCE I10/IR6 Throughflow sections in the southeast Indian Ocean. Part 2: velocity and transport. Deep-Sea Res. II 49, 1363–1389.
Steiger, R.H., Jäger, E., 1977. Subcommission on geochronology: convention on the use of decay constants in geo- and cosmochronology. Earth Planet. Sci. Lett. 36, 359–362.
Stoll, H.M., Vance, D., Arevalos, A., 2007. Records of the Nd isotope composition of seawater from the Bay of Bengal: implications for the impact of Northern Hemisphere cooling on ITCZ movement. Earth Planet. Sci. Lett. 255 (1–2), 213–228.
Stumpf, R., Frank, M., Schönfeld, J., Haley, B.A., 2010. Late Quaternary variability of Mediterranean outflow water from radiogenic Nd and Pb isotopes. Quat. Sci. Rev. 29, 2462–2472. http://dx.doi.org/10.1016/j.quascirev.2010.06.021.
Stumpf, R., Frank, M., Schönfeld, J., Haley, B.A., 2011. Climatically driven changes in sediment supply on the SW Iberian shelf since the Last Glacial Maximum. Earth Planet. Sci. Lett. 312, 80–90. http://dx.doi.org/10.1016/j.quascirev.2011.10.002.
Svensson, A., Andersen, K.K., Bigler, M., Clausen, H.B., Dahl-Jensen, D., Davies, S.M., Johnsen, S.J., Muscheler, R., Rasmussen, S.O., Röthlisberger, R., Steffensen, J.P., Vinther, Bo.M., 2006. The Greenland Ice Core Chronology 2005, 12–42 ka. Part 2: comparison to other records. Quat. Sci. Rev. 25, 3258–3267.
Tachikawa, K., Toyofuku, T., Basile-Doelsch, I., Delhaye, T., 2013. Microscale neodymium distribution in sedimentary planktonic foraminiferal tests and associated mineral phases. Geochim. Cosmochim. Acta 100, 11–23.
Tanaka, T., Togashi, S., Kamioka, H., Amakawa, H., Kagami, H., Hamamoto, T., Yuhara, M., Orihashi, Y., Yoneda, S., Shimizu, H., Kunimaru, T., Takahashi, K., Yanagi, T., Nakano, T., Fujimaki, H., Shinjo, R., Asahara, Y., Tanimizu, M., Dragusanu, C., 2000. JNdi-1: a neodymium isotopic reference in consistency with LaJolla neodymium. Chem. Geol. 168, 279–281.
Tozuka, T., Qu, T., Masumoto, Y., Yamagata, T., 2009. Impacts of the South China Sea Throughflow on seasonal and interannual variations of the Indonesian Throughflow. Dyn. Atmos. Oceans 47 (1–3), 73–85.
Vance, D., Burton, K., 1999. Neodymium isotopes in planktonic foraminifera: a record of the response of continental weathering and ocean circulation rates to climate change. Earth Planet. Sci. Lett. 173, 365–379.
Vance, D., Scrivner, A.E., Beney, P., Staubwasser, M., Henderson, G.M., Slowey, N.C., 2004. The use of foraminifera as a record of the past neodymium isotope composition of seawater. Paleoceanography 19, PA2009. http://dx.doi.org/10.1029/2003PA000957.
van de Flierdt, T., Robinson, L.F., Adkins, J., 2010. Deep-sea coral aragonite as a recorder for the neodymium isotopic composition of sweater. Geochim. Cosmochim. Acta 74, 6014–6032. http://dx.doi.org/10.1016/j.gca.2010.08.001.
Visser, K., Thunell, R., Stott, L., 2003. Magnitude and timing of temperature change in the Indo-Pacific warm pool during deglaciation. Nature 421, 152–155. http://dx.doi.org/10.1038/nature01297.
Voelker, A.H.L., workshop participants, 2002. Global distribution of centennial-scale records for Marine Isotope Stage (MIS) 3: a database. Quat. Sci. Rev. 21, 1185–1212.
Vroon, P.Z., van Bergen, M.J., Klaver, G.J., White, W.M., 1995. Strontium, neodymium, and lead isotopic and trace-element signatures of the East Indonesian sediments: provenance and implications for Banda Arc magma genesis. Geochim. Cosmochim. Acta 59 (12), 2573–2598.
Wijffels, S.E., Meyers Hautala, G., Morawitz, W.M.L., 1996. The WOCE Indonesian Throughflow repeat hydrography sections: I10 and IR6. Int. WOCE Newslett. 24, 25–28.
Xu, J., Holbourn, A., Kuhnt, W., Jian, Z., Kawamura, H., 2008. Changes in the thermocline structure of the Indonesian outflow during Terminations I and II. Earth Planet. Sci. Lett. 273, 152–162.
Xu, J., Kuhnt, W., Holbourn, A., Regenberg, M., Andersen, N., 2010. Indo-Pacific warm pool variability during the Holocene and Last Glacial Maximum. Paleoceanography 25, PA4230. http://dx.doi.org/10.1029/2010PA001934.
Zuraida, R., Holbourn, A., Nürnberg, D., Kuhnt, W., Dürkop, A., Erichsen, A., 2009. Evidence for Indonesian Throughflow slowdown during Heinrich events 3-5. Paleoceanography 24, PA2205. http://dx.doi.org/10.1029/2008PA001653.